Collective Hydrodynamics of Swimming Microorganisms: Living Fluids

Donald L. Koch[1] and Ganesh Subramanian[2]

[1]School of Chemical and Biomolecular Engineering, Cornell University, Ithaca, New York 14853; email: dlk15@cornell.edu

[2]Engineering Mechanics Unit, JNCASR Bangalore, 560 064 India

Annu. Rev. Fluid Mech. 2011. 43:637–59

First published online as a Review in Advance on September 27, 2010

The *Annual Review of Fluid Mechanics* is online at fluid.annualreviews.org

This article's doi: 10.1146/annurev-fluid-121108-145434

0066-4189/11/0115-0637$20.00

Keywords

suspensions, rheology, stability analysis, low Reynolds number, bacteria, active particles

Abstract

Experimental observations indicate that, at sufficiently high cell densities, swimming bacteria exhibit coordinated motions on length scales (10 to 100 μm) that are large compared with the size of an individual cell but too small to yield significant gravitational or inertial effects. We discuss simulations of hydrodynamically interacting self-propelled particles as well as stability analyses and numerical solutions of averaged equations of motion for low Reynolds number swimmers. It has been found that spontaneous motions can arise in such systems from the coupling between the stresses the bacteria induce in the fluid as they swim and the rotation of the bacteria due to the resulting fluid velocity disturbances.

1. INTRODUCTION

Recent experimental observations indicate that suspensions of swimming bacteria develop coordinated motions on length scales (10 to 100 μm) large compared with the size of an individual bacterium (about 3 μm) when their concentration is sufficiently high that cells interact through their hydrodynamic disturbance fields. These observations have inspired numerical simulations of self-propelled particles interacting through their Stokesian disturbance flows as well as continuum analyses of these living fluids with swimming-induced stresses. Although the theories and simulations may apply to a variety of swimming microorganisms or even engineered microswimmers, we consider them primarily in the context of bacterial suspensions in which most of the existing experimental measurements have been made. We aim to give the reader an appreciation for the current state of knowledge; to suggest areas in which theory, simulation, and experimental work could be better coordinated to gain a firmer understanding of collective motion; and to consider possible new directions in the study of living fluids.

Although they are generally considered to be primitive forms of life, bacteria have rich dynamic and social behaviors. Individual cells of many bacterial species swim through fluids with 1-s periods of straight swimming punctuated by tumbling events of a much shorter 0.1-s duration. This stochastic motion becomes biased in the presence of chemical attractant gradients, allowing the cells to efficiently explore their environments and find nutrients (Berg 2003). Bacteria adapt to their environment, excreting protective macromolecules to form biofilms under adverse conditions and swarming to colonize solid surfaces (see the sidebar, What is the Role of Bacterial Motion in Swarming?). It has recently been appreciated that, at high concentrations, bacteria excrete chemicals that signal their neighbors to change their behavior, a phenomenon known as quorum sensing (Nealson & Hastings 1979, Waters & Bassler 2005). It is intriguing to imagine that bacteria may use hydrodynamics as well as biochemistry to coordinate some of their social behavior although the relative significance of these factors in a natural setting remains an open question.

Swimming microorganisms have long been known to create convective patterns on length scales that are much larger than those considered here. These bioconvective motions, driven by changes in buoyancy imparted to the fluid by the presence of concentration gradients of the microorganisms, were the subject of an earlier review by Pedley & Kessler (1992). Bioconvection occurs when cells have a mean swimming motion upward either because a gravitational

WHAT IS THE ROLE OF BACTERIAL MOTION IN SWARMING?

Nearly close-packed populations of bacteria in thin liquid films propagate across solid surfaces through a process known as swarming. The proximity to the solid surface induces the bacterial cells to produce slime; the slime lowers their friction on the surface, in addition to acting as a surfactant. The cells also develop more flagella and larger sizes to enhance their swimming prowess. Steager et al. (2008) quantified the collective dynamics of swarming *Serratia marcescens* bacteria and found bacterial velocities of approximately 10 μm s^{-1} that were correlated over lengths of approximately 10 μm. Although motility is known to enhance the rate of film spreading, the mechanism for this enhancement is not known. Simple estimates (Berg 1993, Zhang et al. 2010) indicate that the force per unit length generated by bacterial motion is about 20 times smaller than surface tension, even assuming that forces can be transmitted over the width of the swarm region. It has been postulated (Daniels et al. 2006) that Marangoni flows, induced by surface-active biomolecules produced by the cells, might account for the film spreading. [Recent experiments with both the wild-type strain and surfactin-deficient mutant strain of *Bacillus subtilis* appear to confirm this hypothesis (Angelini et al. 2009).]

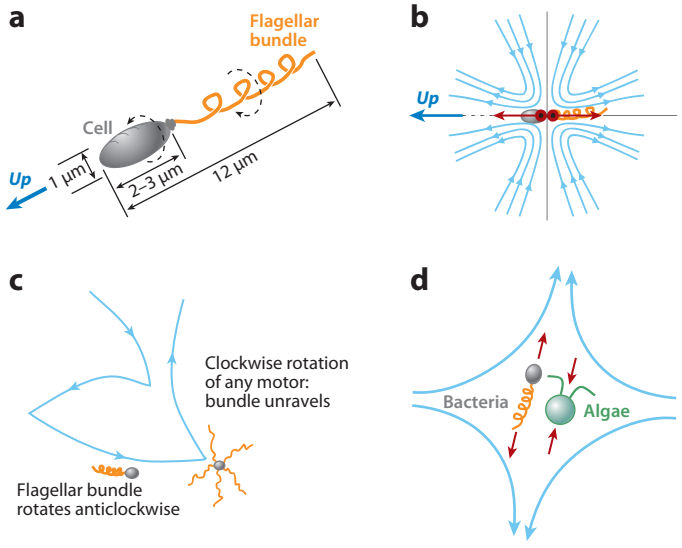

Figure 1

(*a*) A bacterium cell is propelled by the rotation of its screw-like flagellar bundle. (*b*) Dipolar fluid velocity field produced by a swimming bacterium. (*c*) Run-and-tumble motion. (*d*) An extensional fluid motion orients pushers such as bacteria in such a way that their force-dipole (*red arrows*) reinforces the flow, whereas pullers such as algal cells retard the flow.

torque keeps them aligned for upward swimming or because they undergo chemo- or phototaxis. Childress et al. (1975) were among the first to analyze the overturning instability due to the adverse density gradient induced by heavy upward swimming cells. Later, Pedley & Kessler (1990) considered a mechanism of bioconvection associated with the coupling of cell orientation, swimming velocity, and fluid shearing motion in a homogeneous suspension of bottom-heavy cells subject to gyrotactic torques. The critical conditions for the onset of these instabilities are expressed in terms of threshold Rayleigh numbers, and under typical conditions, the critical length scale is of the order of millimeters to centimeters (Pedley & Kessler 1992, Sokolov et al. 2009). Thus the collective motions on 10–100-μm length scales considered in this review are not affected by gravity. A typical Reynolds number for collective bacterial motion (based on a length scale of 40 μm and a velocity of 40 μm s^{-1}) is 1.6×10^{-3}, so inertial effects are also negligible. These estimates suggest that these flows are driven by an instantaneous balance of viscous stresses, pressure, and the stresses induced by approximately neutrally buoyant swimming cells.

Individual *Escherichia coli* or *Bacillus subtilis* cells are spheroidal with lengths of approximately 2–3 μm and diameters of approximately 1 μm (see **Figure 1**). They swim using five to six flagella that are rotated by molecular motors embedded in the cell membrane. The mechanical properties of the flagella have an intrinsic handedness, so that the flagella assemble to form a rigid screw-shaped bundle that turns and propels the cell in a nearly straight path when all the motors rotate in a counterclockwise sense as seen from behind (Kim et al. 2004, Macnab 1977). If one of the motors reverses direction, the bundle unravels and the cell rotates chaotically (i.e., tumbles). Once the motors begin to turn in the same direction again, the bundle reassembles in a new orientation. A typical run lasts for a time $\tau \approx 1$ s for *E. coli* and 0.5 s for *B. subtilis*, and runs are punctuated by brief 0.1-s tumbles (Berg 2003, Wong et al. 1995). Individual cells swimming in a bulk fluid have velocities of approximately 10–30 μm s^{-1} depending on the strain and the conditions under which they were cultured.

The various mechanisms by which microorganisms propel themselves at low Reynolds numbers have been the subject of extensive investigations, and a recent review is given by Lauga & Powers (2009). In most cases the propulsion relies on the anisotropy of the drag force experienced by slender filaments. Slender bodies have a drag coefficient that is approximately twice as large for motion perpendicular to than for motion parallel to their axes. As a result, the rotation of a bacterium's slender screw-like flagella bundle can produce a net hydrodynamic force parallel to its axis of rotation. This force propels the cell and balances the drag force exerted on it at each instant during the swimming motion. The combination of the cell and flagella bundle, viewed as a unit, is thus force-free, and the longest-range hydrodynamic disturbance it produces results from its force-dipole. A cell whose propulsive mechanism is located at its rear is called a pusher. As illustrated in **Figure 1**, it exerts a force-dipole that pushes fluid outward in front and behind it and pulls fluid in from the sides.

Because the forces due to cell swimming are distributed over both the cell body and the flagella bundle, a characteristic length scale for the hydrodynamic force is the combined length $L \approx 12$ μm of the cell plus its flagella bundle. We may therefore expect hydrodynamic coupling between cells to arise when $nL^3 = O(1)$, where n is the number of cells per unit volume. Consistent with this expectation, collective motion has typically been observed when $n = 10^8$ to 10^{10} cells cm^{-3}, corresponding to $nL^3 \approx 0.2$–20. If the cell rotates due to a fluid velocity gradient or an imposed torque while its flagella bundle remains assembled, the forces again extend over both cell and bundle and the relevant length scale is L. Indeed, an estimate of the rotational mobility of *E. coli* in a bulk fluid using the resistive force theory description of the coil (Lauga et al. 2006), and a 3×1 μm spheroidal head, is approximately equal to that of a rod with diameter 1 μm and length 11 μm (Batchelor 1970). We followed the procedure described by Wegener (1981), along with Lighthill's (1976) resistance coefficient for a helical flagellum, to calculate the mobility of the composite object comprising the cell body and flagella. That the relevant hydrodynamic length scale is the combined length of the cell body and the flagellar bundle, rather than the former alone, implies that bacteria such as *E. coli* and *B. subtilis* are essentially athermal objects.

Although our emphasis here is on bacterial cells, we note that any neutrally buoyant microorganism or artificial microswimmer will produce a net force-dipole that then characterizes its interactions on length scales large compared with the cell. Spermatozoa, a pusher that propels by means of a planar undulating flagellum in sufficiently viscous media, can often be concentrated enough to produce collective motion. For example, human spermatozoa is approximately 40 μm long, and normal human semen contains approximately 2×10^7 cells ml^{-1}, yielding $nL^3 \approx 1.3$ (Brennen & Winet 1977, World Health Organization 1999). Because the sperm swimming speed is often a determinant of fertility (Malo et al. 2006), collective motion among sperm cells might be advantageous if it increases the effective cell swimming speed. Algal cells such as *Chlamydomonas reinhardtii* are termed pullers and swim using two flagella that pull the cell from the front. Each cell is approximately spherical with a diameter of 10 μm, and a pair of 10-μm-long flagella is responsible for propulsion, so that the combined size of the cell and flagella is approximately 20 μm. The cell swims at an average speed of approximately 100 μm s^{-1}. When swimming in the dark, without phototactic bias, *C. reinhardtii* has been observed to swim along nearly straight paths for approximately 10 s, followed by abrupt changes in direction (Polin et al. 2009). This is reminiscent of the run-and-tumble motion of bacteria.

On length scales large enough to contain many bacteria, we may view the suspension as an effective continuum. This continuum is a new type of complex fluid, a living fluid whose microstructural elements (the cells) can convert nutrients into mechanical energy to drive fluid flows. Whereas a conventional fluid flows only when imposed gradients of velocity, temperature, pressure, etc., drive it out of equilibrium, this living fluid can develop spontaneous motion in the absence of

imposed gradients using the energy supplied by the swimmers. Some researchers (e.g., Simha & Ramaswamy 2002) have postulated the form of the equations of motion for a living fluid based on general continuum principles, whereas others (e.g., Baskaran & Marchetti 2009, Subramanian & Koch 2009) have derived the equations of motion based on ensemble averaging a detailed microstructural model of hydrodynamically interacting cells. A common feature of these models is the coupling between the fluid motion induced by swimming stresses and the rotation of the swimmers. Continuum equations of motion for living fluids have been analyzed and shown to exhibit novel instabilities not found in passive fluids. The instability threshold has been interpreted as the onset of collective motion. Solutions of the full nonlinear equations of motion have begun to reveal essential features of the predicted collective motion.

The instability of an isotropic suspension of active swimmers involves the coupling of swimmer orientation, fluid flow, and swimming-induced stresses. When a suspension of micrometer-sized swimmers is subject to a simple shear flow with velocity gradients small compared with the inverse of the time τ between tumbles, the orientation distribution is enhanced in the direction of the extensional axis of the shear flow (**Figure 1**). In suspensions of pushers such as *E. coli* and *B. subtilis*, the active stresses of the bacteria in this orientation act to reinforce the imposed extensional motion. In doing so, they make a negative contribution to the viscosity, and Subramanian & Koch (2009) have shown that, at a critical bacteria concentration, this negative active viscosity cancels the viscosity of the suspending liquid. Above this concentration, the bacterial suspension is unstable to fluid velocity disturbances. In a passive fluid, such spontaneous motion would violate thermodynamic principles. However, in a living fluid, cells transform chemical energy into mechanical work driving molecular motors and producing fluid motion. The continuum equations indicate that this motion can occur on length scales much larger than an individual cell length L. On the other hand, the active stresses due to pullers such as the algal species *C. reinhardtii* act to enhance the effective viscosity, in a manner similar to suspensions of passive particles, and an isotropic suspension of such microorganisms is predicted to be stable.

In this article, we first review the experimental evidence for collective bacterial motion. Then in Section 3 we discuss continuum theories for cells swimming in bulk fluids with hydrodynamic interactions. Section 4 reviews simulations of a collection of hydrodynamically interacting self-propelled particles. Section 5 emphasizes future directions.

2. EXPERIMENTAL OBSERVATIONS

Experimental evidence for collective dynamics in suspensions of swimming bacteria has been obtained in the form of observations of the motion of cells and freely suspended colloidal particles, measurement of the forces exerted on colloidal particles in optical traps, determination of the enhanced diffusion of chemical tracers in the presence of bacteria, and inferences about the suspension viscosity based on the rate of decay of imposed fluid motions and the drag on rotating colloidal particles. These measurements have been conducted in thin liquid films on solid (agar) surfaces, in thin freely suspended soap films, and in three-dimensional fluid domains enclosed in microfluidic wells. Most of the observations are for the bacterial species *E. coli* and *B. subtilis*, which are pushers (as described in Section 1) with a combined cell and flagella bundle length of $L \approx 12$ μm, a cell diameter of $d \approx 1$ μm, typical swimming speeds of 10–30 μm s^{-1}, and times between successive tumbles of the order of 1 s.

The first observations of the collective motion of bacteria were obtained by Mendelson et al. (1999) in a thin liquid film of *B. subtilis* swimming on an agar surface. They observed the motion of cells and 1-μm-diameter colloidal particles. Rather than swimming in random uncorrelated directions, the cell motions were correlated over spatial distances of approximately 10–100 μm.

The authors identified and characterized coherent motions consisting of vortices and jets. The motion of the cells and colloidal beads was strongly influenced by the hydration of the agar.

Whereas Mendelson et al. artificially induced cells to swim near an agar surface by enhancing the hydration of the film, bacteria are naturally capable of moving across solid surfaces, within thin liquid films, and the phenomenon is known as swarming (see the sidebar, What is the Role of Bacterial Motion in Swarming?). Steager et al. (2008) observed the swarming velocities of *Serratia marcescens* and characterized the variation of the swarming velocity and two-point velocity correlation length with distance from the edge of the film. The length of the *S. marcescens* cells (5–10 μm) and the high cell density made it impossible for Steager et al. to observe the velocity of individual cells. Instead, the authors developed an image analysis algorithm for the determination of the mean velocity of the cells in an observation window. The mechanism by which cells move in a swarm differs from that in bulk fluid. The cells are confined by the solid surface below, and their motion may also be inhibited by adsorbed macromolecules acting to immobilize the gas-liquid interface (Zhang et al. 2010). In addition, the cell density is high enough that steric effects may enforce local alignment. Observations of rafts of cells with intertwined flagella have led some to postulate that cell motion is aided by transmission of stresses through direct flagellar contact at least in the bacterial species *Proteus mirabilis* (Jones et al. 2004).

Wu & Libchaber (2000) were the first to report collective motion in a suspension of swimming bacteria (*E. coli*) in the absence of a nearby solid boundary. The study was performed on a bacterial suspension in a soap film with a thickness of approximately 10 μm. Soap films have been widely used in studies of two-dimensional turbulence, and it is expected that Marangoni stresses in these films may resist dilatational flows at the gas-liquid interface, while allowing surface shearing flows. As a result, it is thought that flows on length scales large compared with the film thickness are two dimensional and incompressible (Couder et al. 1989). We note that the relevant length scales for bacterial suspension flows range from 1 to 100 μm, which bracket the film thickness. Wu & Libchaber (2000) found 10-μm colloidal beads to execute a diffusive motion over long time intervals with an effective hydrodynamic diffusivity that increased approximately linearly with bacteria concentration for $nL^3 \approx 10$–90, reaching a value of approximately 100 $\mu m^2\ s^{-1}$ at $nL^3 \approx 90$. This effective diffusivity was much larger than the particle's Brownian diffusivity (approximately 0.1 $\mu m^2\ s^{-1}$). Although colloidal beads are commonly used as fluid tracers, the beads in this study were comparable in size to L, so they would not act as point tracers. This was indicated by the fact that the authors observed an approximate doubling of the diffusivity when the bead size was reduced to 4.5 μm.

Sokolov et al. (2007) observed the velocities and orientations of *B. subtilis* cells in a soap-film experiment. The film thickness was approximately 1 μm, so the induced fluid motion may have been nearly two dimensional in this case. The authors developed a scheme to alter the bacterial concentration without encountering issues related to variations in the suspension preparation. They applied a current to a metallic ring within the film, thereby lowering the pH in its vicinity and inducing the bacteria caught within the ring to swim inward and increase their concentration. Examples of the bacterial velocity and orientation fields measured in one such experiment are illustrated in **Figure 2**. Sokolov et al. (2007) observed that the root-mean-square velocity of the bacteria increased in a smooth monotonic fashion with the number of bacteria per unit area, n_a, growing from 15 $\mu m\ s^{-1}$ to 50 $\mu m\ s^{-1}$ over the concentration range $n_a L^2 = 3$–9. On the other hand, the correlation length for two-point measurements of the bacterial velocity grew abruptly from approximately 5 to 20 μm at $n_a L^2 \approx 4$. Although the estimated values of $n_a L^2$ are suggestive of excluded volume effects, possibly leading to local nematic order, the cell orientation field in **Figure 2** shows no strong spatial correlations of orientation. The abrupt increase in the correlation length may then indicate a threshold for instability of an isotropic suspension of bacteria.

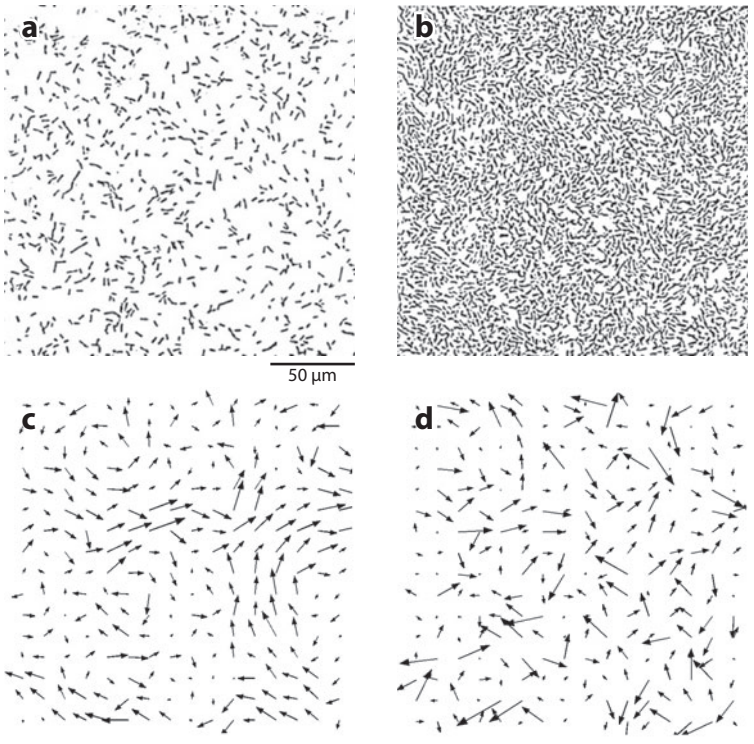

Figure 2

Observations of collective bacteria motion by Sokolov et al. (2007). Bacteria images for $n_a L^2 = 1.7$ (*a*) and 5.6 (*b*), vector bacterial velocity (*c*) and orientation (*d*) fields for $n_a L^2 = 5.6$. Figure reprinted with permission from Sokolov et al. *Phys. Rev. Lett.* 98:158102 (2007). Copyright (2007) by the American Physical Society.

Sokolov et al. found that the correlation between the orientations of the bacterial cells and their velocities increased as one increased the magnitude of the bacterium velocity. Theories (Saintillan & Shelley 2008a,b; Subramanian & Koch 2009; Subramanian et al. 2010) of swimmer suspensions assume the swimmers rotate in a manner similar to passive elongated particles. This assumption leads to an instability arising from the coupling of velocity and orientation perturbations wherein bacterial orientation density is enhanced at an angle of 45° to the direction of the flow. This angle yields a relatively small value (0.2) for the correlation function defined by Sokolov et al. (2007) and is thus consistent with their measurements in regions of low fluid velocity. In the presence of high-amplitude shearing motions (which may lead to high bacterial velocities), elongated particles align with the streamlines of the flow, and this is again consistent with authors' observation of high velocity-orientation correlations in such regions.

The first observations of collective bacterial motion in a three-dimensional fluid domain were by Dombrowski et al. (2004). The primary emphasis of this study was on the bioconvection resulting from the chemotaxis of aerobic *B. subtilis* toward the oxygen-rich region near the gas-liquid interface of a sessile drop. However, the authors found vortical motions to persist even at the interface of a pendant drop, implying that this observed coherent motion may have arisen because of effects unrelated to buoyancy. Subsequent studies (Chen et al. 2007, Leptos et al. 2009, Soni et al. 2003, Wu et al. 2006) have used cylindrical microfluidic wells ranging in depth from

150 to 1,500 μm that are large enough to leave the bacterial motions unconfined and small enough to exclude buoyancy effects.

Soni et al. (2003) measured the temporal correlation of the force acting on a 3-μm-diameter bead held nearly fixed in an optical trap in suspensions of *E. coli*. For a small enough bead and large aspect ratio (L/d) of the bacterium plus flagella, this could be regarded as yielding a two-time Eulerian fluid velocity correlation. However, the results may have been affected to an extent by direct collisions between bacteria and beads. Although the suspension was contained in a three-dimensional domain, the trap was located only 5 μm from a solid wall. The measured force correlation time was found to increase from 0.18 to 0.51 and 1.3 s as the bacterial concentration was increased from $nL^3 = 0.018$ to 0.18 and 1.8.

Wu et al. (2006) measured the diffusivity of *E. coli* as a function of the bacterial concentration in a three-dimensional fluid domain. The diffusivity increased from 50 $\mu m^2\ s^{-1}$ in the dilute limit to 100 $\mu m^2\ s^{-1}$ for $nL^3 = 0.18$, an increase that might be attributed to the onset of an instability. A larger increase in the diffusivity from 450 $\mu m^2\ s^{-1}$ to 1,150 $\mu m^2\ s^{-1}$ was observed for a smooth swimming mutant that did not tumble but underwent a gradual change of orientation due to imperfections of the flagella bundle. This observation is consistent with the theoretical prediction that the rate of decorrelation of bacterium orientation limits the magnitude of the destabilizing active stresses (Subramanian & Koch 2009). Kim & Breuer (2004) observed that motile *E. coli* enhanced the diffusivity of a chemical tracer, being transported in the cross-stream direction of a microchannel flow, from the molecular value of 2 $\mu m^2\ s^{-1}$ to a value of 8 $\mu m^2\ s^{-1}$ at $nL^3 = 3.6$. The enhancement is less than that seen for colloidal beads by Wu & Libchaber (2000) or for bacteria by Wu et al. (2006), and this may be related to the high shear rates ($>1\ s^{-1}$) associated with the microchannel flow. Flow-alignment induced at shear rates higher than the inverse tumbling time could limit the ability of a bacterium to interact with and enhance disturbance flows. This may account for the relatively modest enhancement of diffusion observed. More recently, Leptos et al. (2009) have observed the diffusivity of a 2-μm-diameter colloidal bead to increase from 0.23 $\mu m^2\ s^{-1}$ to 1.8 $\mu m^2\ s^{-1}$ in a suspension of *C. reinhardtii* with $nL^3 = 0.17$. This effect is again considerably weaker than that observed in quiescent suspensions of pushers and is consistent with the theoretical prediction of an isotropic suspension of pullers being stable.

Chen et al. (2007) measured the correlations between the displacements of two colloidal beads separated by a distance r and found a weak, but long-ranged correlation over distances $r = 10$–100 μm and times of 1–10 s comparable with the scales over which bacteria velocities have been found to remain correlated. The authors' interpretation of their results was in terms of small-amplitude hydrodynamic fluctuations of velocity and bacteria concentration in a stable suspension and was based on a model developed by Lau & Lubensky (2009). This model contains a bacteria velocity relative to the fluid that is proportional to the divergence of the bacterial stress leading in turn to longer ranged fluctuations than would be expected for the equations described in Section 3. This relative velocity seems to result from the erroneous assumption that stresses associated with the swimming motion are transmitted only through the fluid phase and not also through particle stresslets induced by the fluid motion. It is possible that the long-ranged fluid motions observed in these experiments are a manifestation of the hydrodynamic instability discussed in Section 3.

Sokolov & Aranson (2009) measured the viscosity of a 200-μm-thick film of *B. subtilis* suspension, surrounded by gas on either side, using two methods. First, they extracted the viscosity from the rate of decay of an imposed vortical motion. In this case, they waited until the velocity of the vortex was 200–500 $\mu m\ s^{-1}$ or smaller before analyzing the decay and extracting the viscosity. The delay in the measurement was to ensure that only the slowest decaying mode of fluid motion remained and, furthermore, that the velocity gradient was small enough for the suspension to

exhibit a Newtonian response. The suspension viscosity was observed to decrease dramatically with increasing bacteria concentration, reaching a minimum value less than 20% of the pure fluid viscosity at $nL^3 = 18$, before increasing again. In the second experiment, the authors extracted a viscosity from the lag between the orientation of a magnetic particle and a rotating magnetic field, and observed a similar trend. The authors varied the swimming speed of the aerobic bacteria by progressively exposing them to higher concentrations of N_2. Faster swimming bacteria led to larger reductions in viscosity, in qualitative agreement with the theoretical prediction that the active stress is proportional to the bacteria's swimming speed (Saintillan & Shelley 2008a,b; Simha & Ramaswamy 2002; Subramanian & Koch 2009; Subramanian et al. 2010). It would be interesting in this experiment to test for the possibility of a shear-rate-dependent viscosity by varying the rotation rate of the magnetic field at a fixed bacterial concentration. Whereas suspensions of passive Brownian rods shear thin, bacterial suspensions are expected to shear thicken as the bacteria become more flow-aligned.

Although spontaneous motion can arise in bacterial suspensions even in the absence of chemical gradients, it seems likely that gradients of chemical attractants that induce chemotactic motion of the bacteria may lead to new mechanisms of instability. The experiment of Sokolov et al. (2009) provides evidence in this regard. In the experiment, aerobic *B. subtilis* suspensions were contained in liquid films with varying thicknesses. In films thinner than approximately 200 μm, the oxygen concentration was relatively uniform across the film thickness, and the bacteria exhibited a two-dimensional coherent motion in the plane of the film. For film thicknesses of approximately 400 μm or larger, oxygen was strongly depleted in the midsection of the film. Under these conditions, three-dimensional convective patterns were observed, apparently triggered by the tendency of the *B. subtilis* cells to swim toward the oxygen-rich region at the fluid-gas interface. The observations suggest that swimming stresses associated with this chemotactic motion can yield a new type of hydrodynamic instability.

The experimental studies reviewed above provide a rich picture of the range of behavior that constitutes spontaneous collective motion in bacterial suspensions. However, for the purpose of testing theories and numerical simulations, it would be valuable to have a single comprehensive study of a well characterized system. For example, would the minimum viscosity, the onset of long-ranged bacterial velocity correlations, and the onset of long-ranged fluid velocity correlations occur at the same bacterial concentration if these properties were all measured in the same experiment? A quantitative comparison of different experiments with one another, and with theory, is made difficult because the concentration of the bacteria is often not known very accurately. In addition, the swimming speed of an individual bacterium is sensitive to the way the cells are cultured. Providing measurements of the root-mean-square bacteria velocity and/or diffusivity in a dilute suspension of bacteria cultured under the same conditions as a concentrated suspension, as done by Wu et al. (2006), would provide vital information to the theoretician. Theories of active matter have assumed cells to rotate in a manner similar to passive particles and have used simple arguments to estimate the hydrodynamic stresses the cells induce. It would be valuable to test these assumptions by observing cell orientation in an imposed flow, on the one hand, and the fluid velocity disturbance produced by a single cell, on the other. Observations of fluid flow above bacterial carpets, consisting of cells adsorbed to a solid surface, suggest that hydrodynamics can couple with the orientations of flagella even when the cells do not rotate (Darnton et al. 2004, Kim & Breuer 2008). If such a phenomenon persists even when the cells are freely suspended, it should be characterized and incorporated into models.

As a primary purpose of cell motility is to allow cells to explore their chemical environments, additional experiments exploring convective motion in chemoattractant gradients would be desirable. A simpler setting in which to search for chemogradient-induced instabilities would be one

in which the attractant gradient is produced by flowing attractant and buffer solutions in channels on opposite sides of a microfluidic well in a hydrogel (Cheng et al. 2007, Kalinin et al. 2009). For chemoattractants that are not consumed by the cells, the chemical gradient is constant (at least in the absence of convective motions) and can therefore be controlled by the experimenter.

At high concentrations, bacteria can produce chemical signals that affect their neighbors. Most of the studies noted above have not attempted to determine if such chemical signaling might coexist with hydrodynamic interactions. An exception in this regard is the study by Soni et al. (2003), who noted the possible role played by chemical signaling; the introduction of a drug that could influence cell signaling reduced the collective motion in their experiments. A more systematic study, perhaps using genetic manipulation to turn on chemical signaling, would be valuable. In systems in which bacteria do produce chemical attractants for neighboring bacteria, dense clusters and rings of bacteria have been observed (Budrene & Berg 1991, 1995). Mathematical models that include reaction, diffusion, and chemotaxis but exclude hydrodynamic flows predict that the cell density develops singularities (Brenner et al. 1998). It seems likely that swimming-induced convection could play a role in modifying these dense regions of self-attracting bacteria.

3. CONTINUUM THEORIES

The initial interest in modeling systems of interacting self-propelled particles, in the absence of external fields, arose in the physics community. The primary motivation appears to have been the collective dynamics observed in numerical simulations of a minimal swimmer model first proposed by Vicsek et al. (1995). The model, similar to those typically used to simulate equilibrium phase transitions (Chaikin & Lubensky 2000), involves an ad hoc specification of local swimmer interactions—a swimmer attempts, on average, to align its velocity with that of its neighbors. The resulting dynamics lead to a nonequilibrium order-disorder transition, above a critical concentration, even in two dimensions. The order parameter being the average velocity, the emergence of an ordered phase, a flock, implies collective swimming on length scales much larger than an individual swimmer. The theories explaining the transition are broad in scope in their attempt to encompass flocking phenomena across species (Grégoire & Chaté 2004, Toner & Tu 1995, Toner et al. 2005). Hydrodynamic interactions between swimmers are neglected in these theories, so the collective swimming predicted, in a manner reminiscent of equilibrium systems, is an emergent phenomenon arising solely from primitive short-range aligning interactions between swimmers.

An isolated swimming bacterium executes a run-and-tumble motion in a quiescent fluid. Whereas the bacterium orientation changes almost impulsively, and by a large amount, during a tumble (the average change is approximately 68°), it also changes continuously during a run. The latter changes may arise from small-amplitude athermal shape fluctuations of the propelling flagellar bundle, and the resulting stochastic motion is modeled as a rotary diffusion (Berg 1993). Apart from such intrinsic orientation decorrelation mechanisms, a bacterium in a suspension may reorient due to excluded volume constraints (at sufficiently high concentrations), hydrodynamic interactions, and in response to inhomogeneous concentration fields of chemicals, either added externally, or secreted by other bacteria. All such interactions must be incorporated in a complete theoretical framework for a suspension of swimming bacteria. At low concentrations and in the absence of chemoattractants, however, interactions between swimming bacteria are primarily hydrodynamic in nature. For the small Reynolds numbers relevant to bacterial suspensions, the velocity field due to an isolated bacterium exhibits a slow $O(1/r^2)$ decay characteristic of a force-dipole (Kim & Karrila 1991); the resulting long-range hydrodynamic interactions in a suspension of such bacteria should fundamentally alter any flocking tendency arising from local short-range interactions. This was first recognized by Simha & Ramaswamy (2002), who proposed a set of

continuum field equations governing the hydrodynamics of an orientationally ordered suspension of inertialess swimmers. From a linear stability analysis, the authors showed that, unlike passive systems, an initial state with either polar or nematic order in such a suspension is unstable to long-wavelength orientation fluctuations. The assumption of orientational order without an external field may have been motivated by an interest in the stability of the ordered phase predicted by theories for flocking, although the short-range interactions in these theories (the driving force for nematic order) play no role in the long-wavelength hydrodynamic instability. The existence of such an instability has since been confirmed via simulations (Saintillan & Shelley 2007).

Tumbling and rotary diffusion are expected to drive the orientation distribution in a bacterial suspension toward isotropy on scales larger than a single bacterium, at least for concentrations small enough that excluded volume interactions do not lead to significant alignment. Thus it is the stability of the isotropic state that is of relevance to a bacterial suspension. In contrast to the nematic phase examined by Simha & Ramaswamy (2002), which remained unstable for suspensions of both pullers and pushers, the isotropic state, first examined by Saintillan & Shelley (2008a,b), was found to be linearly unstable only for a suspension of pushers. This is an important finding as it makes a crucial distinction between the large-scale dynamics emerging from differing propulsion mechanisms at the scale of an individual swimmer; the prediction has found support in the recent simulations of Underhill et al. (2008). None of the above theoretical efforts, however, accounts for the aforementioned orientation decorrelation mechanisms pertinent to a swimming bacterium. For instance, both Simha & Ramaswamy (2002) and Saintillan & Shelley (2008a) assume spatial-diffusion relaxation mechanisms, in which case the relaxation rates become asymptotically weak relative to the rate of destabilization in the limit of long wavelengths. As a result, a suspension of swimmers is predicted to remain unstable at any nonzero concentration. This prediction seems to be at odds with the study of Wu et al. (2006), who found that an enhancement of translational diffusion of bacteria above that associated with individual swimmers only occurs above a critical bacterial concentration. Because tumbling and rotary diffusion lead to orientation decorrelation even in a quiescent medium, the rates of relaxation evidently do not depend on the wavelength of any imposed small-amplitude perturbation. This then leads to a finite threshold concentration for instability.

Via a linear stability analysis in the long-wavelength limit, Subramanian & Koch (2009) derived an expression for the critical concentration for instability in a bacterial suspension. In what follows, we summarize the principal elements of this analysis, starting from the coarse-grained equations that govern the motion of the bacterial suspension on sufficiently large length and time scales. The relevant variables are the ensemble-averaged velocity ($\boldsymbol{u}(\boldsymbol{x}, t)$) and pressure fields ($p(\boldsymbol{x}, t)$), and the probability density ($\Omega(\boldsymbol{x}, \boldsymbol{p}, t)$) governing the position ($\boldsymbol{x}$) and orientation ($\boldsymbol{p}$) of a swimming bacterium, which satisfy the following set of equations:

$$\nabla \cdot \boldsymbol{u} = 0, \tag{1}$$

$$-\nabla p + \mu \nabla^2 \boldsymbol{u} + \nabla \cdot \boldsymbol{\sigma}^B = \boldsymbol{0}, \tag{2}$$

$$\frac{\partial \Omega}{\partial t} + (U\boldsymbol{p} + \boldsymbol{u}) \cdot \nabla_x \Omega + \nabla_p \cdot (\dot{\boldsymbol{p}} \Omega) - D_r \nabla_p^2 \Omega + \frac{1}{\tau}\left(\Omega - \frac{1}{4\pi}\int \Omega d\boldsymbol{p}'\right) = 0. \tag{3}$$

Equation 1 accounts for the medium incompressibility, and Equation 2 represents an instantaneous balance of the viscous and bacterial stresses arising from the neglect of inertia. According to Equation 3, $\Omega(\boldsymbol{x}, \boldsymbol{p}, t)$, in addition to being convected with the sum of the free swimming velocity $U\boldsymbol{p}$ and the fluid velocity field $\boldsymbol{u}$, also changes because of rotary diffusion, tumbling, and a rotation

($\dot{\boldsymbol{p}}$) by the ensemble-averaged fluid velocity field. For a slender bacterium such as *E. coli*, the latter is given by

$$\dot{\boldsymbol{p}} = \boldsymbol{\omega} \cdot \boldsymbol{p} + (\boldsymbol{I} - \boldsymbol{pp}) \cdot (\boldsymbol{e} \cdot \boldsymbol{p}), \tag{4}$$

where $\boldsymbol{\omega}$ and $\boldsymbol{e}$ are respectively the local vorticity and rate of strain tensors associated with the fluid velocity field (Kim & Karrila 1991).The characteristic time scales associated with the tumbling and rotary diffusion processes are τ and D_r^{-1}, respectively, and we have neglected any correlation between the pre- and post-tumble orientations (see Berg 1993); ∇_p here is the gradient operator over the unit sphere. The equations for an active nematic suspension would be similar to those presented above, but with an equation for the director field $\boldsymbol{n}(\boldsymbol{x}, t)$ replacing that for the orientation distribution $\Omega(\boldsymbol{x}, \boldsymbol{p}, t)$ (Simha & Ramaswamy 2002).

The bacterial stress in Equation 2 drives the instability and is given by

$$\boldsymbol{\sigma}^B = -C(n\mu UL^2)\left\langle \boldsymbol{pp} - \frac{1}{3}\boldsymbol{I} \right\rangle, \tag{5}$$

where $\langle\cdot\rangle$ denotes an orientational average weighted by the orientation distribution $\Omega(\boldsymbol{x}, \boldsymbol{p}, t)$. The stress arises because of an orientational anisotropy of the intrinsic force-dipoles and was originally proposed in this form by Simha & Ramaswamy (2002) based on symmetry arguments. The constant C is given by

$$C = \int_{-\frac{L}{2}}^{\frac{L}{2}} s f^i(s) ds, \tag{6}$$

where s is a coordinate along the bacterium swimming axis, and $f^i(s)\boldsymbol{p}$ is the axial force density exerted by a swimming bacterium. The value of C is thus dependent on the details of the swimming mechanism with $C > 0$ (< 0) for pushers (pullers). The suspension is unstable only for pushers, i.e., $C > 0$.

Linearizing the above system of equations about an isotropic base state and considering sinusoidal spatial variations of the fluid velocity, pressure, and the bacterial orientation distribution, a long-wavelength analysis indicates that perturbations to the quiescent state of independently swimming bacteria grow above a threshold concentration, which is a function solely of parameters characterizing the swimming motion of an isolated bacterium:

$$(nL^3)_{\text{crit}} = \frac{1}{C}\left[\frac{5L}{U\tau} + \frac{30LD_r}{U}\right]. \tag{7}$$

For long wavelengths, the nonlocal nature of the bacterial stress due to the swimming motion is not important, and the destabilization arises because of an essentially stationary distribution of bacteria reorienting in response to the local extensional flow associated with the velocity perturbation. The excess of bacterium orientations along the extensional axis then produces an active bacterial stress that reinforces the fluid velocity perturbation (see **Figure 1**). The anisotropy of the orientation distribution and bacterial stress is, at linear order, proportional to the product of the imposed velocity gradient and a relaxation time associated with the twin mechanisms of rotary diffusion and tumbling. The localized nature of the stress, and its linear dependence on the imposed flow, allows an interpretation of the instability as resulting from a negative bacterial contribution to the viscosity. The instability sets in when the negative viscosity associated with the bacteria's swimming-induced force-dipoles negates the stabilizing effect of the solvent viscosity. Quantifying the above argument, the anisotropy is $O(\dot{\gamma}\tau_r) \cdot O(Cn\mu UL^2)$, where the shear rate $\dot{\gamma} \sim O(ku')$ and the relaxation time $\tau_r \sim \tau f(\tau D_r)$; k and u' are the wave number and the amplitude of the perturbation, respectively. Equating the divergence of this stress to that of the viscous stress, $\mu k^2 u'$, yields the general form of the stability criterion. The detailed analysis shows that $f(\tau D_r) = \frac{1}{1+6D_r\tau}$

(see Equation 7). Finally, it is worth noting that the imposed fluid velocity perturbation in the analysis, causing a given bacterium to reorient, must be regarded as the cumulative contribution of the slowly decaying anisotropy of dipolar velocity fields of other distant bacteria; the analysis thus reveals the intrinsic instability of an isotropic bacterial suspension on account of long-range hydrodynamic interactions.

The long-wavelength analysis of Subramanian & Koch (2009) for the general case has been complemented by a calculation of the complete spectrum in the absence of rotary diffusion (see Saintillan & Shelley 2008b, Subramanian et al. 2010). The structure of the eigenspectrum in the limit $\tau \to \infty$ is shown in **Figure 3**; this limit corresponds to the absence of intrinsic decorrelation mechanisms, and a swimmer orientation changes only in response to the ambient velocity gradient. The unstable spectrum for any finite tumbling frequency may be obtained by displacing this limiting spectrum along the real-growth-rate axis by an amount $1/\tau$. We note from **Figure 3** that, in the small-wave-number limit, there is a pair of unstable stationary modes. The dominant mode is triggered by the negative viscosity mechanism and determines the critical concentration for instability, whereas the other is a much weaker mode crucially related to the nonlocal nature of the bacterial stress. The two modes coalesce at $k_m = 0.17C(nL^2)$ and branch off the real axis for larger wave numbers. The resulting pair of traveling waves with complex conjugate growth rates continues only until a maximum wave number given by

$$k'_m = 0.57C(nL^2). \tag{8}$$

The existence of an upper bound to the range of unstable wave numbers implies that the finiteness of the domain may act to stabilize the system, a fact relevant to simulations of active swimmer suspensions (see Section 4).

Subramanian et al. (2010) have also determined the modified spectrum in the presence of an imposed chemoattractant gradient for length and time scales on which the bacterial suspension and the imposed gradient remain homogeneous. The nature of the spectrum is altered in a nontrivial manner. The unstable modes are now traveling waves for any finite wave number, and there appears to no longer be an upper bound on the range of unstable wave numbers. On longer time scales, the balance between the chemotactic and diffusive fluxes in a finite domain leads to an inhomogeneous concentration distribution that is expected to modify the stability characteristics on larger length scales.

The above analysis predicts an instability of isotropic suspensions of pushers but indicates that isotropic suspensions of pullers are always stable. Baskaran & Marchetti (2009) have suggested a mechanism by which anisotropic translational diffusion of pullers could lead to an instability involving coupled orientational and bacterial concentration perturbations. Even if one were to accept the relevance of translational diffusion, however, this analysis is flawed. The bacterial concentration perturbations in the theory are driven by a flux proportional to the divergence of $\langle \boldsymbol{pp} \rangle$. This term was obtained by performing a nonconvergent convolution integral between the force-dipole velocity disturbance of a swimmer and the orientation moment [equation 38 of Baskaran & Marchetti's (2009) supplemental material]. In an appropriate ensemble-averaged equation approach, the swimmers' force-dipoles would lead to a solenoidal fluid velocity field driven by a mean active stress.

Although the linear stability analysis of the isotropic state of pushers predicts the critical concentration for the onset of collective swimming, it does not predict a dominant length scale in the unstable regime. This is seen from **Figure 3** in which the growth rate of the dominant stationary mode approaches a shallow maximum in the limit of zero wave number, implying that a broad spectrum of modes, with wave numbers in the interval [0, $O(nL^2)$], may influence the nonlinear evolution of the perturbations. A numerical solution of the continuum field equations

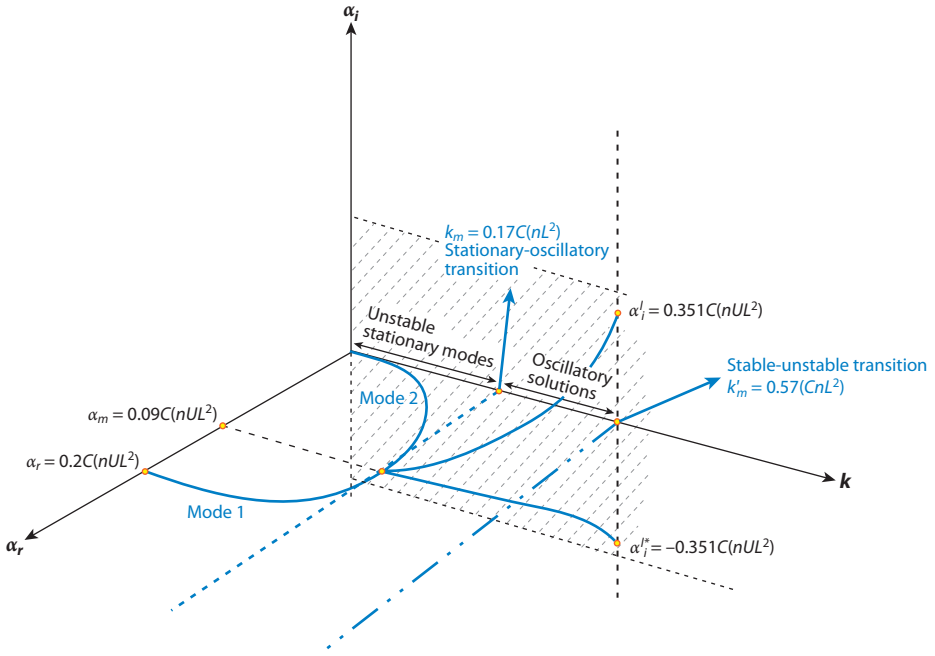

Figure 3

The real (α_r) and imaginary (α_i) parts of the growth rate of fluid velocity modes in a suspension of straight swimmers plotted as a function of the wave number k.

therefore becomes valuable in this regard and should help reveal the nonlinear flow structures, along with the characteristic length and time scales, that dominate the collective swimming regime. A step in this direction has been taken by Saintillan & Shelley (2008b) and Wolgemuth (2008), who have numerically solved the field equations in two dimensions starting from an initial nematic state and an initially isotropic orientation distribution, respectively.

An intriguing result in the simulations of Saintillan & Shelley (2008b) is the appearance of large-amplitude density fluctuations in the nonlinear regime. This result is of particular interest because the unstable modes in the linearized theory arise owing to a coupling of velocity and orientation field fluctuations, implying that an initially homogeneous suspension will retain a constant bacterial number density even as it becomes unstable to fluid velocity and orientation fluctuations. The fluid velocity field being incompressible, any inhomogeneity of the number density can only arise because of swimming and is therefore related to the divergence of $\langle \boldsymbol{p} \rangle$. Such a quantity will only be nonzero if there exists a $\boldsymbol{p}/-\boldsymbol{p}$ bias at the macroscopic level, in other words, a macroscopic polarity fluctuation. Because the dynamics of the instability does not break the $\boldsymbol{p} \leftrightarrow -\boldsymbol{p}$ symmetry, it is reasonable to imagine that an initial condition involving an apolar order at the macroscopic level will not lead to large polarity fluctuations at later times. Thus the observed density fluctuations in the simulations of Saintillan & Shelley (2008b) may have arisen because of polarity fluctuations seeded by the initial condition. The continued presence of large-amplitude density fluctuations nevertheless implies that the initial seed of large polarity does not die away, in turn suggesting that the spatially homogeneous state may not be a global attractor for all initial conditions. This might, however, arise because of the neglect of tumbling and rotary diffusion, which may act to attenuate any initial polarity fluctuations. Indeed, all simulations of active swimmers to date are restricted to

the case of straight swimmers, in which case orientation decorrelation arises solely on account of hydrodynamic interactions. The incorporation of nonhydrodynamic relaxation mechanisms may help address the relevance of number density fluctuations to the collective swimming regime.

Even for concentrations below the threshold value given by Equation 7, bacterial suspensions may exhibit novel rheological characteristics. For instance, implicit in the stability analysis of Subramanian & Koch (2009) is the prediction that the viscosity of a bacterial suspension must, in sharp contrast to passive particle suspensions, decrease with increasing nL^3 up until the onset of instability. Furthermore, over a range of flow amplitudes in which the intrinsic swimming behavior of a bacterium is expected to remain unaltered, bacterial suspensions must exhibit a shear-thickening rheology; this is again in contrast to most complex fluids, which exhibit a shear-thinning rheology close to equilibrium (Larson 1999). The shear thickening is expected to arise because, although slender bacteria tend to align with the local extensional axis of a weak imposed simple shear flow, they must approach flow-alignment in stronger flows. The alignment must decrease their effect on the flow and thereby lead to an increased viscosity. The nontrivial effects of (swimming) activity on the rheology of suspensions of active particles have been pointed out, in a rather general context, by Hatwalne et al. (2004).

There have been recent attempts to determine the nonlinear rheological properties, including normal stress differences, of active suspensions (Saintillan 2010). The calculation bears a close resemblance to earlier analyses for suspensions of dipolar Brownian orientable particles (see Brenner 1972); the bacterium orientation distribution, under the combined influence of flow and relaxation processes, is first obtained and then used to determine the bacterial stress contribution. Although the distribution of bacterium orientations is similar to that of Brownian fibers for similar amplitudes of the imposed flow, an analogy between passive Brownian fibers and bacteria does not hold for the stress contributions associated with the relaxation process. This is because athermal relaxation processes in bacterial suspensions must conform to a torque-free constraint (the constraint that, for instance, causes the bacterium head and the flagellar bundle to rotate in opposite senses about the swimming axis). As a consequence, the magnitude and nature of the stress contributions associated with such relaxation processes must differ fundamentally from the corresponding entropic stress contributions that arise from Brownian torques. The active swimming stresses that dominate the rheology reported by Saintillan (2010) at high shear rates would be correct, but the Brownian stress contribution, which becomes increasingly important at small shear rates, is not appropriate to athermal bacteria.

Theories in the physics literature (see Ramaswamy & Simha 2006, Ramaswamy et al. 2003, Simha & Ramaswamy 2002) have pointed out profound differences between the hydrodynamic fluctuations in orientationally ordered active and passive systems. For instance, Simha & Ramaswamy (2002) have shown that surprisingly long-ranged concentration fluctuations arise in suspensions of self-propelled particles with a macroscopic polar order. The difference in the nature of correlations arises because the stress driving the flow in an active suspension is proportional to $\boldsymbol{nn}$ (see Equation 5), whereas the corresponding passive stress, being associated with an (elastic) free energy functional, involves spatial gradients of the director field $\boldsymbol{n}$. The active stress thus drives a much stronger flow in the long-wavelength limit, in turn leading to long-range director field and concentration fluctuations. It must be emphasized that these fluctuations are a characteristic of the stable regime and differ from those that arise because of a saturation of the linear instability discussed above. It would be desirable to carry out simulations, for instance, along the lines of Saintillan & Shelley (2007) (see Section 4), to clarify the nature of the fluctuations in the stable and unstable regimes. Such simulations must, however, incorporate swimmer-swimmer interactions leading to a nematic potential so that a stable active nematic state can be observed. Furthermore, they must include stochastic orientation decorrelation mechanisms, as it is such

random reorientation events, mediated by excluded volume interactions, that serve as a source term for the director field fluctuations in the stable regime.

An issue that emerges from the above discussion is to predict under what conditions will orientational order, either polar or nematic, emerge at the macroscopic level due to local interactions between microscopic polar swimmers (bacteria). Neighboring swimmers may align due to hydrodynamic interactions or on account of excluded volume constraints. The latter come into play in swarming films of bacteria and for sufficiently concentrated suspensions ($n \geq 10^{10}$ cells ml^{-1}). Recent theories, although restricted to two dimensions, have attempted to incorporate excluded volume interactions both via a Boltzmann-like collision integral (Aranson et al. 2007, Bertin et al. 2006) and via an Onsager excluded volume potential (Baskaran & Marchetti 2008b) in the kinetic equation for the probability density (see Equation 3); the underlying motivation is to explore the stability and dynamics of the ordered phase that forms as a result. The nature of the macroscopic order appears to depend on the shape of the swimmer, and a collection of symmetrical rod-like swimmers with solely excluded volume interactions only exhibits a bulk nematic order (see Baskaran & Marchetti 2008a). In their simulations of hydrodynamically interacting spherical squirmers, Ishikawa et al. (2008) have observed long-range orientation correlations for a certain type of squirmer (see Section 4 for details). On the other hand, in simulations of force-free dumbbells (see Hernández-Ortiz et al. 2009, Underhill et al. 2008), in which the near-field hydrodynamics differs from that for a squirmer, hydrodynamic interactions prevent rather than promote nematic order. Thus it appears that any mechanism that might lead to a macroscopic ordered state is likely to depend on the details of how bacteria swim in close proximity to one another, and these detailed close-range interactions need to be observed directly in experiments.

Continuum theories thus far have largely been restricted to exploring collective dynamics in an unbounded domain. An issue that deserves attention is the boundary conditions that must complement the field equations for finite-sized domains and the spatial extent of the region in which such conditions might alter the predicted bulk dynamics. This is particularly important in the context of microfluidic applications. The few efforts that explore the motion of active fluids in simple geometries (Edwards & Yeomans 2009) employ rather ad hoc boundary conditions for the bacterium orientation field motivated in part by similar conditions for passive nematics (Larson 1999). A formulation of appropriate boundary conditions may need to account for the variety of behaviors observed for bacteria swimming close to surfaces. These include swimming in circles (Lauga et al. 2006), swimming along curved trajectories (DiLuzio et al. 2005), upstream motion in an imposed shear flow (Hill et al. 2007), and a tendency to either recoil (Cisneros et al. 2006) or to change to a parallel swimming mode (Galajda et al. 2007) in the presence of an obstacle. Experiments highlighting the interaction of bacteria with nearby surfaces may also offer clues as to how the intrinsic swimming dynamics (including tumbling and rotary diffusion) might be modified at high concentrations and may thereby help in arriving at a sensible model for the excluded volume interactions.

4. SIMULATIONS

Simulations of hydrodynamically interacting self-propelled particles provide opportunities to (*a*) test continuum theories under circumstances in which the relevant parameters can be controlled more precisely than in experiments, (*b*) reveal fluctuations that result from the discrete nature of the swimmers, (*c*) explore interactions of swimmers with boundaries that have not yet been incorporated into continuum theories, and (*d*) reveal the effects of short-range hydrodynamic interactions. The simulations discussed below include a variety of swimmer geometries and

propulsion mechanisms. Two common features of the work to date are that the swimmers are force-free, as is appropriate for neutrally buoyant cells, but lack a mechanism such as tumbling by means of which an isolated cell's orientation could decorrelate even in the absence of interactions between swimmers.

The first simulation study exhibiting the long-range collective hydrodynamic motion in a suspension of self-propelled particles is that of Saintillan & Shelley (2007). The particles in this study are slender rods, and an actuating shear stress distribution on either the fore (puller) or aft (pusher) part of a rod causes it to swim. The hydrodynamic interactions are modeled using viscous slender-body theory (see Batchelor 1970, Mackaplow & Shaqfeh 1998). The simulations were restricted to initial orientation fields with polar or apolar (nematic) order, and the swimmer concentrations ranged over two orders of magnitude ($nL^3 \sim 0.4$–40). In all cases, the initial orientationally ordered state was found to be unstable. The suspension evolves toward a state that is isotropic on large length scales, although orientational correlations persist at smaller scales. This observation confirms the theoretical predictions of Simha & Ramaswamy (2002) that an active suspension (of pushers or pullers) with either polar or nematic order is unstable to long-wavelength orientation fluctuations. Although the theory considered a nematic potential modeled as a director diffusivity (acting to damp orientation fluctuations) that is absent in the simulations, the growth rate of the instability at large wavelengths was independent of the director diffusivity.

The results of Saintillan & Shelley (2007) show that, in the saturated state for a suspension of pushers, the orientational decorrelation can be modeled with a hydrodynamically induced rotary diffusivity D_r that grows as nL^2U. Although a rotary diffusivity that grows linearly with swimmer concentration could arise from pairwise interactions in a dilute stable suspension, the coefficient observed in Saintillan & Shelley's simulations is about two orders of magnitude larger than that calculated by Subramanian & Koch (2009) for pairwise interactions. The reason for this discrepancy is unclear. The translational diffusion D of the swimmers was found to be well predicted by a Taylor dispersion process [$D = U^2/(6D_r)$], suggesting that swimming, modulated by orientational decorrelation, was the primary determinant of the mean-square displacement of the rods.

Hernández-Ortiz et al. (2005, 2007) developed a fast multipole method of simulating hydrodynamically interacting swimming dumbbells. Each dumbbell consisted of a pair of beads linked by a rigid rod such that the center-to-center distance L between the beads was three times the bead radius. The swimmers interacted hydrodynamically via point-force velocity disturbance fields centered at the beads and via excluded volume interactions. The swimming motion was driven by a phantom flagellum that acted on one of the beads, leading the two beads of a single dumbbell to exert equal and opposite forces on the fluid. As a result, a swimming dumbbell acted as a force-dipole on large length scales. The method may be used with periodic boundary conditions in all directions, or with one or more solid boundaries.

Underhill et al. (2008) have used the above algorithm to simulate an isotropic suspension of swimming dumbbells in a spatially periodic cubic domain. The hydrodynamic diffusivity of passive non-Brownian fluid tracers was found to grow as $H^{0.63}$ with the domain size H in suspensions of pushers for the range $H/L = 10$–50; on the other hand, the diffusivity was much smaller in suspensions of pullers. The fluid velocity variance in the former case was, however, a weak function of H and of the same order as the square of the swimming speed. These observations are consistent with the postulate that fluid mixing arises from large-scale coherent motions associated with the instability in an isotropic suspension of pushers (discussed in Section 3). A criterion for the instability of straight swimmers in a finite domain may be obtained by replacing the maximum unstable wave number k'_m (see Equation 8 in Section 3) by $2\pi/H$, leading to the threshold concentration

for instability $(nL^3)_{crit} = 2\pi/[0.57C(H/L)]$. Neglecting the hydrodynamic interaction between the beads constituting a dumbbell, the force-dipole coefficient (see Equation 5 in Section 3) is $C = 2\pi$, implying $H/L > 1.75/(nL^3)$ for instability. Because $nL^3 = (3/5\pi)$ in all the simulations, the entire range of domain sizes simulated allows for the existence of unstable modes, although the wavelength of the unstable mode approaches the domain size for the smallest domains. Thus the suspensions of pushers simulated are expected to develop fluid motion on length scales much larger than L. Furthermore, the observed $O(U)$ amplitude of the fluid velocity fluctuations implies that the fluid velocity gradient is $O(U/\lambda)$, where λ is the wavelength of the fluid motion. This fluid shear rate will cause a swimmer to rotate through an order one fraction of its Jeffery orbit in the shear, as it swims across a wavelength, and as a result it provides an optimal opportunity for an excess swimmer orientation density to develop near the extensional axis of the flow as discussed by Subramanian & Koch (2009). Underhill et al.'s observation that the tracer diffusivity induced by pullers is small and nearly independent of domain size, under conditions that yield large diffusivities for pushers, constitutes an important confirmation of the theoretical prediction that the former system is stable and the latter is unstable. A surprising feature of the simulations of pushers is that the correlation length and time of the fluid velocity, while dependent on the domain size, remain smaller than H and H/U, respectively.

Hernández-Ortiz et al. (2009) simulated suspensions of swimming dumbbells with gap-averaged concentrations of $\langle n \rangle L^3 \approx 0.01$–$0.6$ confined between planar rigid walls with gaps of $5L$–$10L$. The majority of the dumbbells swam in thin layers near the walls with a much smaller concentration in the bulk suspension away from the walls. That both pullers and pushers, whose interaction with their respective hydrodynamic images is of an opposite nature, formed thin layers near the walls suggests that the mechanism leading to the layers was predominantly ballistic impingement rather than sustained hydrodynamic dumbbell-wall interactions. Simulations that included hydrodynamic interactions between dumbbells had significantly larger bulk concentrations than those that did not. Thus the hydrodynamic interactions among the dumbbells may have largely accounted for the desorption from the wall layer. It would be interesting to know what role tumbling, which was omitted from these simulations, might play in such a desorption process. Under the conditions simulated, the hydrodynamic flow consisted of vortical motions on a length scale comparable with the wall spacing. However, these motions could be explained by a superposition of the hydrodynamic flows by independent swimmers in the presence of walls and are not a manifestation of collective dynamics. Indeed, the flow field of even an isolated swimmer interacting with a wall contains closed streamlines, and any inference of collective swimming merely based on visual evidence of large closed streamline regions (vortices) may be subject to error. Hernández-Ortiz et al. (2009) noted that the apparent collective motion reported earlier by Hernández-Ortiz et al. (2005) resulted from the omission of excluded volume interactions among the dumbbells and the unrealistically large velocities that resulted from close encounters.

Ishikawa et al. (2008) have simulated a suspension of hydrodynamically interacting spherical particles known as squirmers. The swimming in this case occurs owing to a specified tangential velocity distribution on the particle surface; the surface velocity is a superposition of two fundamental modes—a fore-aft symmetric stresslet singularity and a potential dipole singularity. A squirmer may provide an accurate model of eukaryotic cells such as *Opalina* and *Paramecium caudatum*, which swim by the waving motion of the many cilia that cover their surfaces (Brennen & Winet 1977, Ishikawa & Hota 2006), but it is not expected to model the short-range interactions of flagellated bacteria. The simulations make use of Stokesian dynamics (Brady & Bossis 1988, Durlofsky et al. 1987), an approach developed for passive particles that incorporates many-body

force-dipole interactions as well as an exact pairwise description of short-range hydrodynamic interactions. By considering a spherical model, Ishikawa et al. (2008) forego the possibility that the swimmers' orientation distribution can be deformed by their interaction with a simple shear flow; in turn, this precludes the hydrodynamic instability of nonspherical pushers thought to cause the collective motion observed in the simulations of Underhill et al. (2008). The most striking results for the squirmer model occur for pullers and specifically for a unit ratio of the stresslet and potential dipole coefficients. In this case, there is a large excess of close pairs with parallel orientations, implying that short-range hydrodynamic interactions may lead to polar order. It should, however, be noted that the behavior of squirmers is sensitive to the model parameters, and these have not been tuned to reflect any specific microorganism. Indeed, the observation that the puller rods simulated by Saintillan & Shelley (2007) show a deficit of close pairs, whereas the puller squirmers of Ishikawa et al. (2008) show an excess, indicates the importance of seeking an accurate model of the short-range interactions and geometry. Mehandia & Nott (2008) have also adapted the Stokesian dynamics method to simulate a suspension of swimmers in an attempt to rigorously incorporate short-range hydrodynamic interactions. However, the approach is again restricted to spherical swimmers and uses a surface velocity boundary condition that is not representative of a flagellated swimmer.

It would be desirable to develop a new generation of swimmer simulations that aims to accurately model the short-range interactions of cells while maintaining reasonable computational efficiency. As noted in Section 1, the hydrodynamic resistance to rotation of a bacterium swimming with a flagellar bundle is strongly influenced by the flagella, so it is essential to model the nonspherical nature of the swimmer. A slender-body treatment with a no-slip head and a tail having a specified slip velocity, which drives the swimming, is a reasonable starting point. It is known that the counter-rotation of the tail and head causes cells to swim in circles adjacent to walls (Lauga et al. 2006), and this motion, which could be incorporated in a slender-body treatment by distributing rotlets along the cell axis, may also influence short-range cell-cell interactions. The finite thickness of the cell and flagellar bundle may play a role in creating nematic ordering at high concentrations. This may be implemented by simply allowing for an excluded volume of a finite thickness along with slender-body hydrodynamics. The effect of finite thickness on hydrodynamic interactions could also be simulated using a Stokesian dynamics formulation for spheroids such as that developed by Claeys & Brady (1993a–c) in the context of passive particle suspensions.

Simulations of active swimmers have thus far been restricted to the case in which the swimmer orientation changes only due to hydrodynamic interactions. Although useful as a base case in isolating the role of hydrodynamics, one must include nonhydrodynamic relaxation mechanisms to simulate the dynamics of a bacterial suspension. The mechanisms most relevant to a swimming bacterium are rotary diffusion and tumbling, both of which decorrelate its orientation on characteristic time scales of 1–3 s. These mechanisms play an essential role in allowing a sufficiently dilute isotropic bacterial suspension to be stable. In rigid-rod suspensions, Brownian rotary diffusion, in acting to eliminate any flow-induced orientation anisotropy, leads to an entropic stress; the stress arises from the restoring action of Brownian torques (see Hinch & Leal 1972). However, as discussed in Section 3, rotary diffusion of a bacterium has an athermal origin and must therefore conform to a torque-free constraint. As argued by Subramanian & Koch (2009), this is likely to make the athermal analog of the entropic stress much smaller. In a simulation of slender rods, this could be accomplished by choosing a new orientation for the rod without allowing for any fluid flow associated with the rod rotation. The increment in orientation could be small for rotary diffusion or large for a tumble. In the case of swimmers with finite thickness, this artifice could, however, lead to particle-particle overlaps. An alternative method would be to specify a force distribution, having no net force or torque, that nonetheless induces a rotation of a swimmer.

5. FUTURE ISSUES

Herein we summarize some of the main issues that need to be addressed in the future. There is a clear need to conduct experiments on a well characterized system and, in addition, to be able to monitor multiple quantities in a given experiment, for instance, the effective viscosity, velocity, and orientation fields as a function of the bacterial concentration. This should help isolate, in an unambiguous manner, the critical concentration for the onset of collective dynamics, and thereby forge a connection between experimental measurements and linear stability theories that predict the threshold for collective motion. The theoretical formulations need to account for the presence of boundaries, and the boundary conditions must capture the variety of behavior exhibited by bacteria swimming in the vicinity of solid surfaces. Simulations must use model swimmers that accurately reflect the short-range interactions of real microorganisms and, in addition, incorporate the nonhydrodynamic orientation decorrelation processes, exhibited by bacteria like *E. coli* and *B. subtilis* typically used in experimental studies. Finally, studies of collective motion in these systems need to account for the presence of both imposed and induced chemoattractant fields, and hence the combined effects of hydrodynamics and cell-cell signaling on the large-scale dynamics of the system.

DISCLOSURE STATEMENT

The authors are not aware of any affiliations, memberships, funding, or financial holdings that might be perceived as affecting the objectivity of this review.

ACKNOWLEDGMENTS

This work was supported by NSF grant CBET-0730579.

LITERATURE CITED

Angelini TE, Roper M, Kolter R, Weitz DA, Brenner MP. 2009. *Bacillus subtilis* spreads by surfing on waves of surfactant. *Proc. Natl. Acad. Sci. USA* 106:18109–13

Aranson I, Sokolov A, Kessler J, Goldstein R. 2007. Model for dynamical coherence in thin films of self-propelled microorganisms. *Phys. Rev. E* 75:040901

Baskaran A, Marchetti M. 2008a. Enhanced diffusion and ordering of self-propelled rods. *Phys. Rev. Lett.* 101:268101

Baskaran A, Marchetti MC. 2008b. Hydrodynamics of self-propelled hard rods. *Phys. Rev. E* 77:011920

Baskaran A, Marchetti M. 2009. Statistical mechanics and hydrodynamics of bacterial suspensions. *Proc. Natl. Acad. Sci. USA* 106:15567–72

Batchelor GK. 1970. Slender-body theory for particles of arbitrary cross-section in Stokes flow. *J. Fluid Mech.* 44:419–40

Berg HC. 1993. *Random Walks in Biology*. Princeton, NJ: Princeton Univ. Press

Berg HC. 2003. E. coli *in Motion*. New York: Springer

Bertin E, Droz M, Gregoire G. 2006. Boltzmann and hydrodynamic description for self-propelled particles. *Phys. Rev. E* 74:022101

Brady JF, Bossis G. 1988. Stokesian dynamics. *Annu. Rev. Fluid Mech.* 20:111–57

Brennen C, Winet H. 1977. Fluid mechanics of propulsion by cilia and flagella. *Annu. Rev. Fluid Mech.* 9:339–98

Brenner H. 1972. Rheology of a dilute suspension of axisymmetric Brownian particles. *Int. J. Multiphase Flow* 1:195–341

Brenner MP, Levitov LS, Budrene EO. 1998. Physical mechanisms for chemotactic pattern formation by bacteria. *Biophys. J.* 74:1677–93

Budrene EO, Berg HC. 1991. Complex patterns formed by motile cells of *Escherichia coli*. *Nature* 349:630–33
Budrene EO, Berg HC. 1995. Dynamics of formation of symmetrical patterns by chemotactic bacteria. *Nature* 376:49–53
Chaikin P, Lubensky T. 2000. *Principles of Condensed Matter Physics*. Cambridge, UK: Cambridge Univ. Press
Chen DTN, Lau AWC, Hough LA, Islam MF, Goulian M, et al. 2007. Fluctuations and rheology in active bacterial suspensions. *Phys. Rev. Lett.* 99:148302
Cheng S, Heilman S, Wasserman M, Archer S, Shuler M, Wu M. 2007. A hydrogel-based microfluidic device for the studies of directed cell migration. *Lab Chip* 7:763–69
Childress S, Levandowsky M, Spiegel EA. 1975. Pattern formation in a suspension of swimming microorganisms: equations and stability theory. *J. Fluid Mech.* 69:591–613
Cisneros L, Dombrowski C, Goldstein R, Kessler J. 2006. Reversal of bacterial locomotion at an obstacle. *Phys. Rev. E* 73:030901
Claeys IL, Brady JF. 1993a. Suspensions of prolate spheroids in Stokes flow. Part 1. Dynamics of a finite number of particles in an unbounded fluid. *J. Fluid Mech.* 251:411–42
Claeys IL, Brady JF. 1993b. Suspensions of prolate spheroids in Stokes flow. Part 2. Statistically homogeneous dispersions. *J. Fluid Mech.* 251:443–77
Claeys IL, Brady JF. 1993c. Suspensions of prolate spheroids in Stokes flow. Part 3. Hydrodynamic transport properties of crystalline dispersions. *J. Fluid Mech.* 251:479–500
Couder Y, Chomaz JM, Rabaud M. 1989. On the hydrodynamics of soap films. *Physica D* 37:384–405
Daniels R, Reynaert S, Hoekstra H, Verreth C, Janssens J, et al. 2006. Quorum signal molecules as biosurfactants affecting swarming in *Rhizobium etli*. *Proc. Natl. Acad. Sci. USA* 103:14965–70
Darnton N, Turner L, Breuer K, Berg HC. 2004. Moving fluid with bacterial carpets. *Biophys. J.* 86:1863–70
DiLuzio W, Turner L, Mayer M, Garstecki P, Weibel D, et al. 2005. *Escherichia coli* swim on the right-hand side. *Nature* 435:1271–74
Dombrowski C, Cisneros L, Chatkaew S, Goldstein RE, Kessler JO. 2004. Self-concentration and large-scale coherence in bacterial dynamics. *Phys. Rev. Lett.* 93:098103
Durlofsky L, Brady JF, Bossis G. 1987. Dynamic simulation of hydrodynamically interacting particles. *J. Fluid Mech.* 180:21–49
Edwards S, Yeomans J. 2009. Spontaneous flow states in active nematics: a unified picture. *Europhys. Lett.* 85:18008
Galajda P, Keymer J, Chaikin P, Austin R. 2007. A wall of funnels concentrates swimming bacteria. *J. Bacteriol.* 189:8704–7
Grégoire G, Chaté H. 2004. Onset of collective and cohesive motion. *Phys. Rev. Lett.* 92:025702
Hatwalne Y, Ramaswamy S, Rao M, Simha RA. 2004. Rheology of active-particle suspensions. *Phys. Rev. Lett.* 92:118101
Hernández-Ortiz JP, de Pablo JJ, Graham MD. 2007. Fast computation of many-particle hydrodynamic and electrostatic interactions in a confined geometry. *Phys. Rev. Lett.* 98:140602
Hernández-Ortiz JP, Stoltz CG, Graham MD. 2005. Transport and collective dynamics in suspensions of confined swimming particles. *Phys. Rev. Lett.* 95:204501
Hernández-Ortiz JP, Underhill PT, Graham MD. 2009. Dynamics of confined suspensions of swimming particles. *J. Phys. Condens. Matter* 21:204107
Hill J, Kalkanci O, McMurry J, Koser H. 2007. Hydrodynamic surface interactions enable *Escherichia coli* to seek efficient routes to swim upstream. *Phys. Rev. Lett.* 98:068101
Hinch EJ, Leal LG. 1972. The effect of Brownian motion on the rheological properties of a suspension of non-spherical particles. *J. Fluid Mech.* 52:683–712
Ishikawa T, Hota M. 2006. Interaction of two swimming Paramecia. *J. Exp. Biol.* 209:4452–63
Ishikawa T, Locsei JT, Pedley TJ. 2008. Development of coherent structures in concentrated suspensions of swimming model micro-organisms. *J. Fluid Mech.* 615:401–31
Jones BV, Young R, Mahenthiralingam E, Stickler DJ. 2004. Ultrastructure of *Proteus mirabilis* swarmer cell rafts and role of swarming in catheter-associated urinary tract infection. *Infect. Immun.* 72:3941–50
Kalinin YV, Jiang L, Tu Y, Wu M. 2009. Logarithmic sensing in *Escherichia coli* bacterial chemotaxis. *Biophys. J.* 96:2439–48

Kim MJ, Breuer KS. 2004. Enhanced diffusion due to motile bacteria. *Phys. Fluids* 16:L78–81
Kim MJ, Breuer KS. 2008. Microfluidic pump powered by self-organizing bacteria. *Small* 4:111–18
Kim MJ, Kim MJ, Bird JC, Park J, Powers TR, Breuer KS. 2004. Particle image velocimetry experiments on a macro-scale model for bacterial flagellar bundling. *Exp. Fluids* 37:782–88
Kim S, Karrila S. 1991. *Microhydrodynamics*. Boston: Butterworth-Heinemann
Larson R. 1999. *The Structure and Rheology of Complex Fluids*. New York: Oxford Univ. Press
Lau A, Lubensky T. 2009. Fluctuating hydrodynamics and microrheology of a dilute suspension of swimming bacteria. *Phys. Rev. E* 80:011917
Lauga E, DiLuzio WR, Whitesides GM, Stone HA. 2006. Swimming in circles: motion of bacteria near solid boundaries. *Biophys. J.* 90:400–12
Lauga E, Powers TR. 2009. The hydrodynamics of swimming microorganisms. *Rep. Prog. Phys.* 72:096601
Leptos KC, Guasto JS, Gollub JP, Pesci AI, Goldstein RE. 2009. Dynamics of enhanced tracer diffusion in suspensions of swimming eukaryotic microorganisms. *Phys. Rev. Lett.* 103:198103
Lighthill J. 1976. Flagellar hydrodynamics. *SIAM Rev.* 18:161–230
Mackaplow MB, Shaqfeh ESG. 1998. A numerical study of the sedimentation of fibre suspensions. *J. Fluid Mech.* 376:149–82
Macnab R. 1977. Bacterial flagella rotating in bundles: a study in helical geometry. *Proc. Natl. Acad. Sci. USA* 74:221–25
Malo AF, Gomendio M, Garde J, Lang-Lenton B, Soler AJ, Roldan ER. 2006. Sperm design and sperm function. *Biol. Lett.* 2:246–49
Mehandia V, Nott P. 2008. The collective dynamics of self-propelled particles. *J. Fluid Mech.* 595:239–64
Mendelson NH, Bourque A, Wilkening K, Anderson KR, Watkins JC. 1999. Organized cell swimming motions in *Bacillus subtilis* colonies: patterns of short-lived whirls and jets. *J. Bacteriol.* 181:600–9
Nealson KH, Hastings JW. 1979. Bacterial bioluminescence: its control and ecological significance. *Microbiol. Mol. Biol. Rev.* 43:496–518
Pedley TJ, Kessler JO. 1990. A new continuum model for suspensions of gyrotactic micro-organisms. *J. Fluid Mech.* 212:155–82
Pedley TJ, Kessler JO. 1992. Hydrodynamic phenomena in suspensions of swimming microorganisms. *Annu. Rev. Fluid Mech.* 24:313–58
Polin M, Tuval I, Drescher K, Gollub JP, Goldstein RE. 2009. *Chlamydomonas* swims with two "gears" in a eukaryotic version of run-and-tumble locomotion. *Science* 325:487–90
Ramaswamy S, Aditi Simha R, Toner J. 2003. Active nematics on a substrate: giant number fluctuations and long-time tails. *Europhys. Lett.* 62:196–202
Ramaswamy S, Simha RA. 2006. The mechanics of active matter: broken-symmetry hydrodynamics of motile particles and granular layers. *Solid State Commun.* 139:617–22
Saintillan D. 2010. The dilute rheology of swimming suspensions: a simple kinetic model. *Exp. Mech.* In press; doi: 10.1007/s11340-009-9267-0
Saintillan D, Shelley MJ. 2007. Orientational order and instabilities in suspensions of self-locomoting rods. *Phys. Rev. Lett.* 99:058102
Saintillan D, Shelley MJ. 2008a. Instabilities and pattern formation in active particle suspensions: kinetic theory and continuum simulations. *Phys. Rev. Lett.* 100:178103
Saintillan D, Shelley MJ. 2008b. Instabilities, pattern formation, and mixing in active suspensions. *Phys. Fluids* 20:123304
Simha RA, Ramaswamy S. 2002. Hydrodynamic fluctuations and instabilities in ordered suspensions of self-propelled particles. *Phys. Rev. Lett.* 89:058101
Sokolov A, Aranson IS. 2009. Reduction of viscosity in suspension of swimming bacteria. *Phys. Rev. Lett.* 103:148101
Sokolov A, Aranson IS, Kessler JO, Goldstein RE. 2007. Concentration dependence of the collective dynamics of swimming bacteria. *Phys. Rev. Lett.* 98:158102
Sokolov A, Goldstein RE, Feldchtein FI, Aranson IS. 2009. Enhanced mixing and spatial instability in concentrated bacterial suspensions. *Phys. Rev. E* 80:031903
Soni G, Ali BJ, Hatwalne Y, Shivashankar G. 2003. Single particle tracking of correlated bacterial dynamics. *Biophys. J.* 84:2634–37

Steager EB, Kim CB, Kim MJ. 2008. Dynamics of pattern formation in bacterial swarms. *Phys. Fluids* 20:073601
Subramanian G, Koch DL. 2009. Critical bacterial concentration for the onset of collective swimming. *J. Fluid Mech.* 632:359–400
Subramanian G, Koch DL, Fitzgibbon SR. 2010. The stability of a homogeneous suspension of chemotactic bacteria. *Phys. Fluids.* In press
Toner J, Tu Y. 1995. Long-range order in a two-dimensional dynamical *xy* model: How birds fly together. *Phys. Rev. Lett.* 75:4326–29
Toner J, Tu Y, Ramaswamy S. 2005. Hydrodynamics and phases of flocks. *Ann. Phys.* 318:170–244
Underhill PT, Hernández-Ortiz JP, Graham MD. 2008. Diffusion and spatial correlations in suspensions of swimming particles. *Phys. Rev. Lett.* 100:248101
Vicsek T, Czirók A, Ben-Jacob E, Cohen I, Shochet O. 1995. Novel type of phase transition in a system of self-driven particles. *Phys. Rev. Lett.* 75:1226–29
Waters CM, Bassler BL. 2005. Quorum sensing: cell-to-cell communication in bacteria. *Annu. Rev. Cell Dev. Biol.* 21:319–46
Wegener W. 1981. Diffusion coefficients for rigid macromolecules with irregular shapes that allow rotational-translational coupling. *Peptide Sci.* 20:303–26
Wolgemuth C. 2008. Collective swimming and the dynamics of bacterial turbulence. *Biophys. J.* 95:1564–74
Wong L, Johnson M, Zhulin I, Taylor B. 1995. Role of methylation in aerotaxis in *Bacillus subtilis*. *J. Bacteriol.* 177:3985–91
World Health Organization. 1999. *WHO Laboratory Manual for the Examination of Human Semen and Sperm-Cervical Mucus Interaction*. Cambridge, UK: Cambridge Univ. Press
Wu M, Roberts JW, Kim S, Koch DL, DeLisa MP. 2006. Collective bacterial dynamics revealed using a three-dimensional population-scale defocused particle tracking technique. *Appl. Environ. Microbiol.* 72:4987–94
Wu XL, Libchaber A. 2000. Particle diffusion in a quasi-two-dimensional bacterial bath. *Phys. Rev. Lett.* 84:3017–20
Zhang R, Turner L, Berg HC. 2010. The upper surface of an *Escherichia coli* swarm is stationary. *Proc. Natl. Acad. Sci. USA* 107:288–90

Annual Review of
Fluid Mechanics

Volume 43, 2011

Contents

Experimental Studies of Transition to Turbulence in a Pipe
T. Mullin 1

Fish Swimming and Bird/Insect Flight
Theodore Yaotsu Wu 25

Wave Turbulence
Alan C. Newell and Benno Rumpf 59

Transition and Stability of High-Speed Boundary Layers
Alexander Fedorov 79

Fluctuations and Instability in Sedimentation
Élisabeth Guazzelli and John Hinch 97

Shock-Bubble Interactions
Devesh Ranjan, Jason Oakley, and Riccardo Bonazza 117

Fluid-Structure Interaction in Internal Physiological Flows
Matthias Heil and Andrew L. Hazel 141

Numerical Methods for High-Speed Flows
Sergio Pirozzoli 163

Fluid Mechanics of Papermaking
Fredrik Lundell, L. Daniel Söderberg, and P. Henrik Alfredsson 195

Lagrangian Dynamics and Models of the Velocity Gradient Tensor in Turbulent Flows
Charles Meneveau 219

Actuators for Active Flow Control
Louis N. Cattafesta III and Mark Sheplak 247

Fluid Dynamics of Dissolved Polymer Molecules in Confined Geometries
Michael D. Graham 273

Discrete Conservation Properties of Unstructured Mesh Schemes
J. Blair Perot 299

Global Linear Instability
Vassilios Theofilis 319

High–Reynolds Number Wall Turbulence
Alexander J. Smits, Beverley J. McKeon, and Ivan Marusic 353

Scale Interactions in Magnetohydrodynamic Turbulence
Pablo D. Mininni 377

Optical Particle Characterization in Flows
Cameron Tropea 399

Aerodynamic Aspects of Wind Energy Conversion
Jens Nørkær Sørensen 427

Flapping and Bending Bodies Interacting with Fluid Flows
Michael J. Shelley and Jun Zhang 449

Pulse Wave Propagation in the Arterial Tree
Frans N. van de Vosse and Nikos Stergiopulos 467

Mammalian Sperm Motility: Observation and Theory
E.A. Gaffney, H. Gadêlha, D.J. Smith, J.R. Blake, and J.C. Kirkman-Brown 501

Shear-Layer Instabilities: Particle Image Velocimetry Measurements and Implications for Acoustics
Scott C. Morris 529

Rip Currents
Robert A. Dalrymple, Jamie H. MacMahan, Ad J.H.M. Reniers, and Varjola Nelko 551

Planetary Magnetic Fields and Fluid Dynamos
Chris A. Jones 583

Surfactant Effects on Bubble Motion and Bubbly Flows
Shu Takagi and Yoichiro Matsumoto 615

Collective Hydrodynamics of Swimming Microorganisms: Living Fluids
Donald L. Koch and Ganesh Subramanian 637

Aerobreakup of Newtonian and Viscoelastic Liquids
T.G. Theofanous 661

Indexes

Cumulative Index of Contributing Authors, Volumes 1–43 691

Cumulative Index of Chapter Titles, Volumes 1–43 699

Errata

An online log of corrections to *Annual Review of Fluid Mechanics* articles may be found at http://fluid.annualreviews.org/errata.shtml